The Effect of Small-Scale Moisture Variability on Thunderstorm Initiation

TAMMY M. WECKWERTH

Atmospheric Technology Division, National Center for Atmospheric Research, Boulder, Colorado

(Manuscript received 27 December 1999, in final form 3 April 2000)

ABSTRACT

Observations during the Convection and Precipitation/Electrification (CaPE) project illustrate that horizontal convective rolls are capable of providing sufficient forcing to initiate free moist convection. Rolls occurred on the majority of days during CaPE but on only some of those days were they able to trigger thunderstorms. This study was undertaken to ascertain the difference between the two types of roll days: the storm days and the no-storm days. All obvious sounding parameters were examined: stability parameters, midlevel moisture, and vertical wind shear. None of them showed a difference between the storm and no-storm days. This is not surprising in light of recent work showing that soundings within rolls are not representative of the environmental stability unless they happen to be launched into roll updraft branches. This is due to the upward transport of warm, moist air in the roll updraft regions atop which cloud streets and sometimes thunderstorms form. Numerous other parameters examined were also fruitless in identifying any difference between the days. These included surface station measurements, cell motion relative to roll updraft locations, surface topography, and roll circulation strength and depth. The only useful predictor was obtained by modifying the soundings using aircraft data as they were flying across the rolls and sampling moisture contained within the roll updraft branches. Using these roll updraft moisture measurements to recalculate sounding stability parameters provided an effective means of predicting thunderstorm formation.

1. Introduction

Boundary layer forcing has long been known to be a cause of thunderstorm initiation (Byers and Braham 1949; Purdom 1982). Low-level convergence zones shown to be instrumental in producing thunderstorms include gust fronts (e.g., Wilson and Schreiber 1986; Weckwerth and Wakimoto 1992; Rasmussen et al. 2000), sea-breeze fronts (e.g., Byers and Rodebush 1948; Pielke 1974; Fankhauser et al. 1995; Laird et al. 1995), drylines (e.g., Rhea 1966; Hane et al. 1997; Ziegler and Rasmussen 1998), cold fronts (e.g., Shapiro et al. 1985), and stationary convergence zones (e.g., Wilson et al. 1992). This is particularly true if cumulus clouds exist in advance of the approaching convergence zones (e.g., Trier et al. 1991; Wilson and Mueller 1993; Kingsmill 1995). The intersections of these convergence zones with either one another or with horizontal convective rolls create preferred locations for convective development (e.g., Purdom 1982; Wilson and Schreiber 1986; Wilson et al. 1992; Atkins et al. 1995). Rolls consist of counterrotating vortices within the convective boundary layer (e.g., LeMone 1973; Kuettner 1971; Kristovich 1993). Rolls may thus be thought of as a type of boundary layer convergence zone. In addition to interacting boundaries influencing convective development, modeling studies suggest that rolls may initiate deep convection when in proper alignment with internal gravity waves aloft (Balaji and Clark 1988). There have not, however, been any detailed studies of the initiation of thunderstorms by rolls alone.

Crook (1996) used a cloud-resolving model to show that predicting the initiation of thunderstorms along a boundary layer convergence zone is highly dependent upon very accurate estimates of water vapor within and just above the convective boundary layer (CBL). Radiosondes are typically used to initialize such cloud models but Weckwerth et al. (1996) found that radiosondes launched in an environment containing rolls are not representative of the convective potential of that environment unless the soundings are launched within the roll updraft. When they used soundings to predict cloud bases, they found significant overestimates when compared with cloud bases measured by cloud photogrammetric techniques and radars. It is known that cloud streets occur atop roll updraft branches (e.g., Kuettner 1959; LeMone and Pennell 1976; Chlond 1992). Christian and Wakimoto (1989) clearly showed the relationship between radar-observed rolls and cloud locations. Thus it follows that if thunderstorms form along rolls, they will form atop the roll updraft branches. These updraft regions are more moist than the remainder of

Corresponding author address: Dr. Tammy M. Weckwerth, NCAR, P. O. Box 3000, Boulder, CO 80307-3000.
E-mail: tammy@ucar.edu

the roll circulations (e.g., LeMone and Pennell 1976; Reinking et al. 1981). Weckwerth et al. (1996) observed water vapor mixing ratio differences of 1.5–2.5 g kg^{-1} between roll updrafts and downdrafts. Thus, unless the sounding happens to be released within a roll updraft branch, it will not be sampling the air that is forced upward to create the clouds. It is therefore proposed that, even in the absence of boundary layer convergence zones, a single sounding alone will typically not be useful for evaluating the potential for thunderstorm initiation.

Rolls developed practically every day during the Convection and Precipitation/Electrification (CaPE) project in east-central Florida during the summer of 1991 (e.g., Wakimoto and Atkins 1994). They have been shown to form when there is a combination of sensible heat flux and wind shear. Some studies have shown that thermal instability is the dominant roll-forcing mechanism (Kuo 1963; Asai 1970a,b, 1972). Other studies have found that dynamical instability is dominant when rolls form (e.g., Faller 1963; Lilly 1966; Brümmer 1985; Stensrud and Shirer 1988). The majority of roll studies, however, have found that some combination of thermal and dynamical instability must be present for rolls to form (Woodcock 1942; Miura 1986; Grossman 1982; Kristovich 1993; Weckwerth et al. 1997). During CaPE some roll days produced deep moist convection while other roll days did not initiate thunderstorms. *The goal of this study is to ascertain the difference between the two types of days; that is, why did rolls produce deep moist convection on some days but not on other days.*

The CaPE dataset and methodology will be described in section 2. Section 3 will show two characteristic examples: a storm day and a no-storm day. The multitude of parameters examined to address this issue of thunderstorm initiation will be presented in section 4. Section 5 includes a summary and concluding remarks.

2. Methodology

Data collected during the CaPE project show that rolls alone are sometimes sufficient to initiate thunderstorms. Utilizing the National Center for Atmospheric Research's (NCAR) CP-3 and CP-4 Doppler radars (Keeler et al. 1991) and visible satellite imagery, thunderstorm initiation atop roll updraft branches is observed. Thunderstorm initiation is defined as radar reflectivities >35 dB*Z*. These radar and satellite data are also used to verify the lack of low-level forcing from any other boundary layer convergence zones, such as gust fronts, sea-breeze fronts, lake breezes, and river breezes in order to examine the initiation of true airmass thunderstorms due solely to the roll circulations.

Cross-chain Loran Atmospheric Sounding System (CLASS; Lauritsen et al. 1987) radiosondes, and Portable Automated Mesonet (PAM II; Brock et al. 1986) stations are used to measure the environmental thermodynamic parameters. The soundings were edited to remove sensor-arm heating (Cole and Miller 1995) and dry biases known to be a factor with the Vaisala radiosondes (e.g., Cole and Miller 1999; Weckwerth et al. 1999b; Guichard et al. 2000). Vaisala sondes were used exclusively during CaPE. The PAM II surface station data are used to assess and correct the dry biases. The absolute accuracies, that is, absolute uncertainties (precisions) of the sounding mixing ratio and potential temperature measurements made within the CBL are at least 1.5 g kg^{-1} (0.4 g kg^{-1}) and 0.5 K (0.2 K), respectively (Weckwerth et al. 1996). The mixing ratio errors are likely larger due to the unknown errors in the corrections applied. The resulting accuracy and precision values are not yet known.

The University of Wyoming (UW) and NCAR King Air aircraft (e.g., Fankhauser et al. 1985; Rodi et al. 1991) made numerous flights at various levels during roll occurrences. The flights across the rolls within the CBL are used extensively in this study. Moisture biases of the UW King Air were established from intercomparison flights with the NCAR King Air and tower flybys (Fankhauzer et al. 1985). After these corrections are applied, the absolute accuracies (precisions) of the aircraft mixing ratios and potential temperatures are 0.4 g kg^{-1} (0.04 g kg^{-1}) and 0.4 K (0.04 K), respectively (Weckwerth et al. 1996).

Using the entire suite of available instruments, the environmental parameters are measured to ascertain why rolls produced storms on some days but not on other days. Numerous radiosondes were launched prior to and during thunderstorm formation. The calculations of convective inhibition (CIN) and convective available potential energy (CAPE) are used to examine the atmospheric stability. Utilizing both radiosondes and velocity-azimuth display (VAD) radar analyses, the vertical wind shear was observed. Along these same lines, cell motions are examined by looking at time series of plan-position indicator radar reflectivity data. Dual-Doppler analyses obtained from the CP-3 and CP-4 radars are used to compare the roll circulation strength and depth on the different types of days. The PAM II surface station measurements and surface topography are also examined.

Eight days are examined on which radar data confirmed that rolls alone were able to initiate deep moist convection and on which soundings were launched within 1 h of storm initiation. No other low-level convergence features other than rolls were in the region nor was there any large-scale forcing evident. These storms produced radar reflectivities greater than 35 dB*Z*. The storm days analyzed are 15 July, 23 July, 25 July, 27 July, 29 July, 30 July, 2 August, and 7 August 1991. These days are compared with data from five days on which rolls alone did not initiate thunderstorms. The no-storm days are 14 July, 4 August, 6 August, 10 August, and 17 August 1991. As with the storm days, none of these no-storm days exhibit any synoptic-scale influences. The objective of this study is to ascertain why

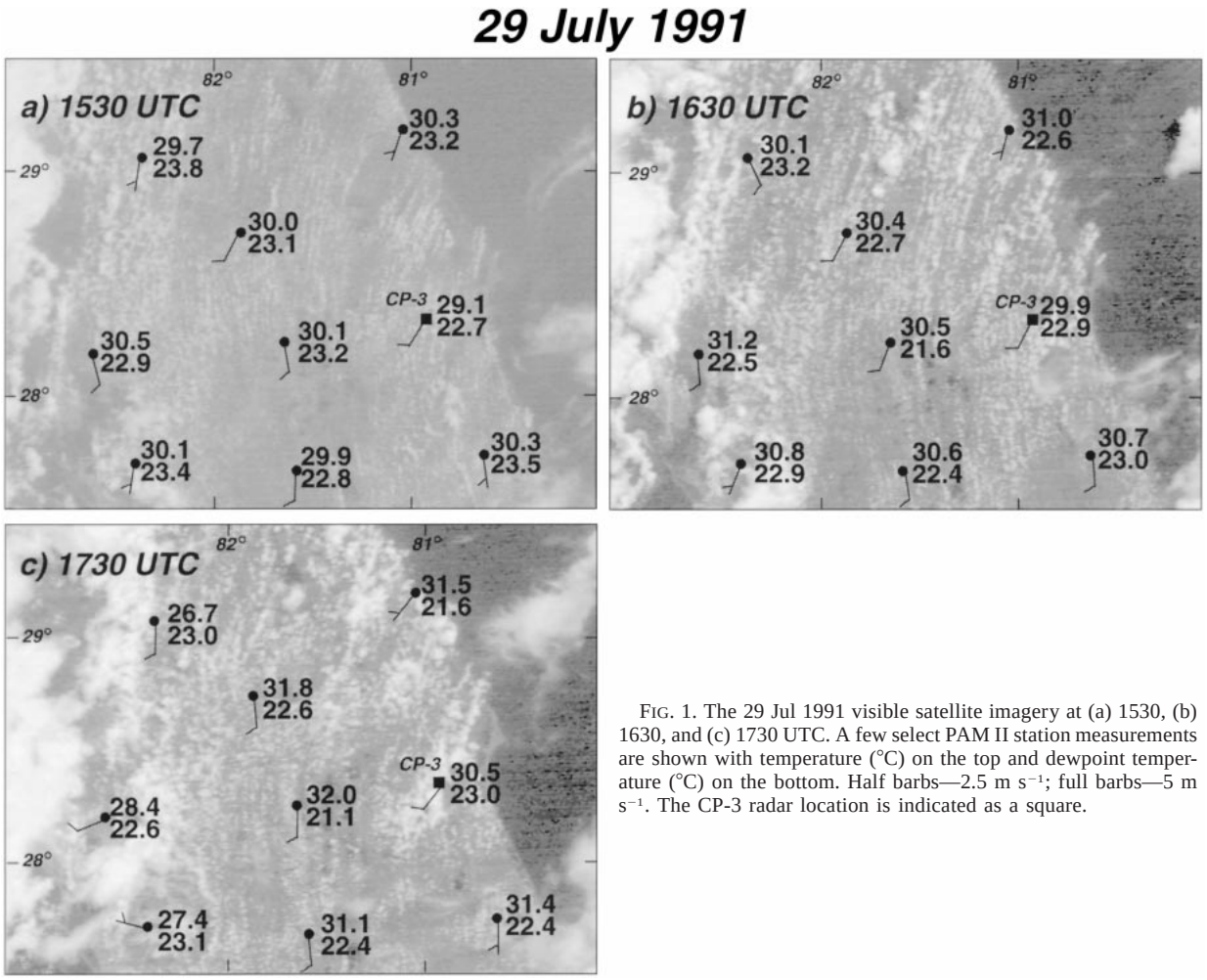

FIG. 1. The 29 Jul 1991 visible satellite imagery at (a) 1530, (b) 1630, and (c) 1730 UTC. A few select PAM II station measurements are shown with temperature (°C) on the top and dewpoint temperature (°C) on the bottom. Half barbs—2.5 m s^{-1}; full barbs—5 m s^{-1}. The CP-3 radar location is indicated as a square.

roll forcing was sufficient to produce storms on some days but not on other days.

3. Characteristic examples

Two days will be shown in detail: 29 July 1991 on which rolls produced thunderstorms and 10 August 1991 on which rolls did not produce storms.

a. Storm day: 29 July 1991

Visible satellite imagery on 29 July is shown in Fig. 1. At 1530 UTC (hereafter, all times will be UTC; UTC = LT + 4 h) cloud streets are apparent across the Florida peninsula (Fig. 1a). The rolls display a north-northeast–south-southwest orientation in the northern portion of the image that changes toward a nearly north–south orientation south of the CP-3 radar. As expected, this orientation is consistent with the wind direction (e.g., Malkus and Riehl 1964). The clouds are shallow and scattered across most of the peninsula. Similarly the low-level CP-3 radar reflectivity field (Fig. 2a) shows north-northeast–south-southwest-oriented fine lines indicating roll updraft branches (Wilson et al. 1994). The cloud streets atop the roll updraft regions are apparent as north-northeast–south-southwest-oriented popcorn cells on the higher-level scan (Fig. 2b).

By 1630 the cloud streets are more pronounced across the entire peninsula (Fig. 1b). Some deeper clouds are beginning to form, in particular, toward the east and south of CP-3 along a small lake-breeze front. The low-level radar reflectivity shows that the boundary layer roll circulations are becoming less linear (Fig. 2c) as the storm-scale circulations are dominating due to the increased convective development (Fig. 2d). Note the continued north-northeast–south-southwest alignment of the echoes aloft as enhanced convection forms atop the rolls 25 km southeast of CP-3.

Figure 1c shows that several storms form near CP-3 by 1730. The previous north-northeast–south-southwest orientation of the rolls is still apparent in the deeper cloud field. Note that no other boundary layer convergence zones (e.g., sea-breeze fronts, gust fronts, or lake-breeze fronts) are apparent near the CP-3 radar. The

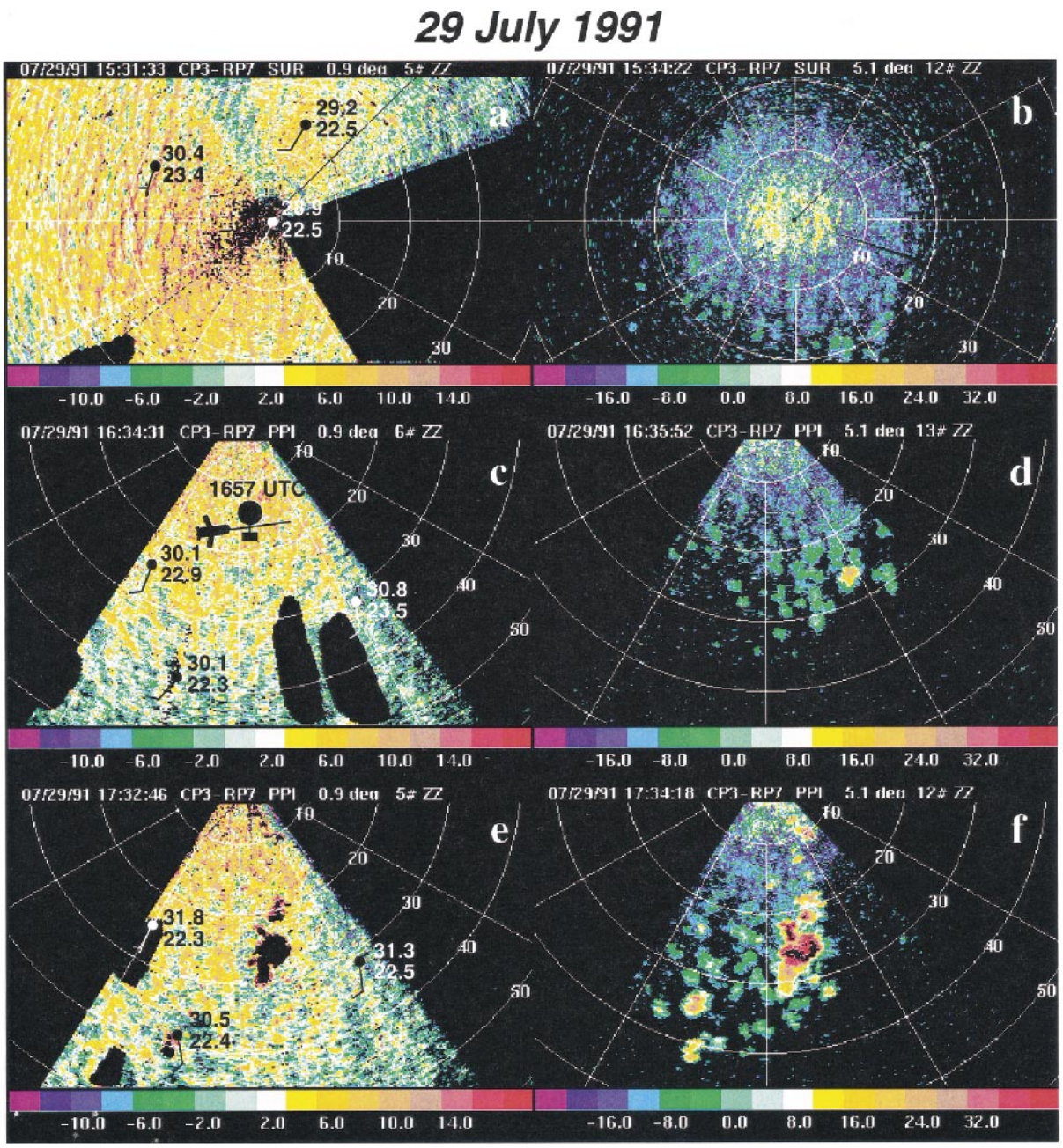

FIG. 2. The 29 Jul 1991 time series of CP-3 C-band radar reflectivities (dBZ_e) showing thunderstorm initiation by rolls with low-level data on the left and upper levels on the right. Second-trip artifacts are removed and appear as black blobs. Black regions within intense echoes are off the scale, which was selected to illustrate the rolls in the CBL and clouds aloft. PAM II station measurements are shown as in Fig. 1. A mobile CLASS radiosonde was launched at 1657 UTC from the location of the balloon in (c). Sounding data will be shown in Fig. 5, along with aircraft data from the cross-roll direction between 1634 and 1717 UTC along the track shown in (c).

small lake-breeze front and associated convection from Fig. 1b had dissipated by this time. The low-level radar reflectivity scans (Figs. 2a, 2c, and 2e) also support this observation that no other boundary layer convergence zones are within the CP-3 domain at the time of thunderstorm initiation. Figure 2e shows that the rolls become less organized as the storms continue to grow (Fig. 2f). Similarly, the other seven storm days examined also showed that rolls alone initiated free moist convection.

b. No-storm day: 10 August 1991

In contrast on 10 August 1991 the rolls do not initiate free convection. East–west cloud streets, oriented along

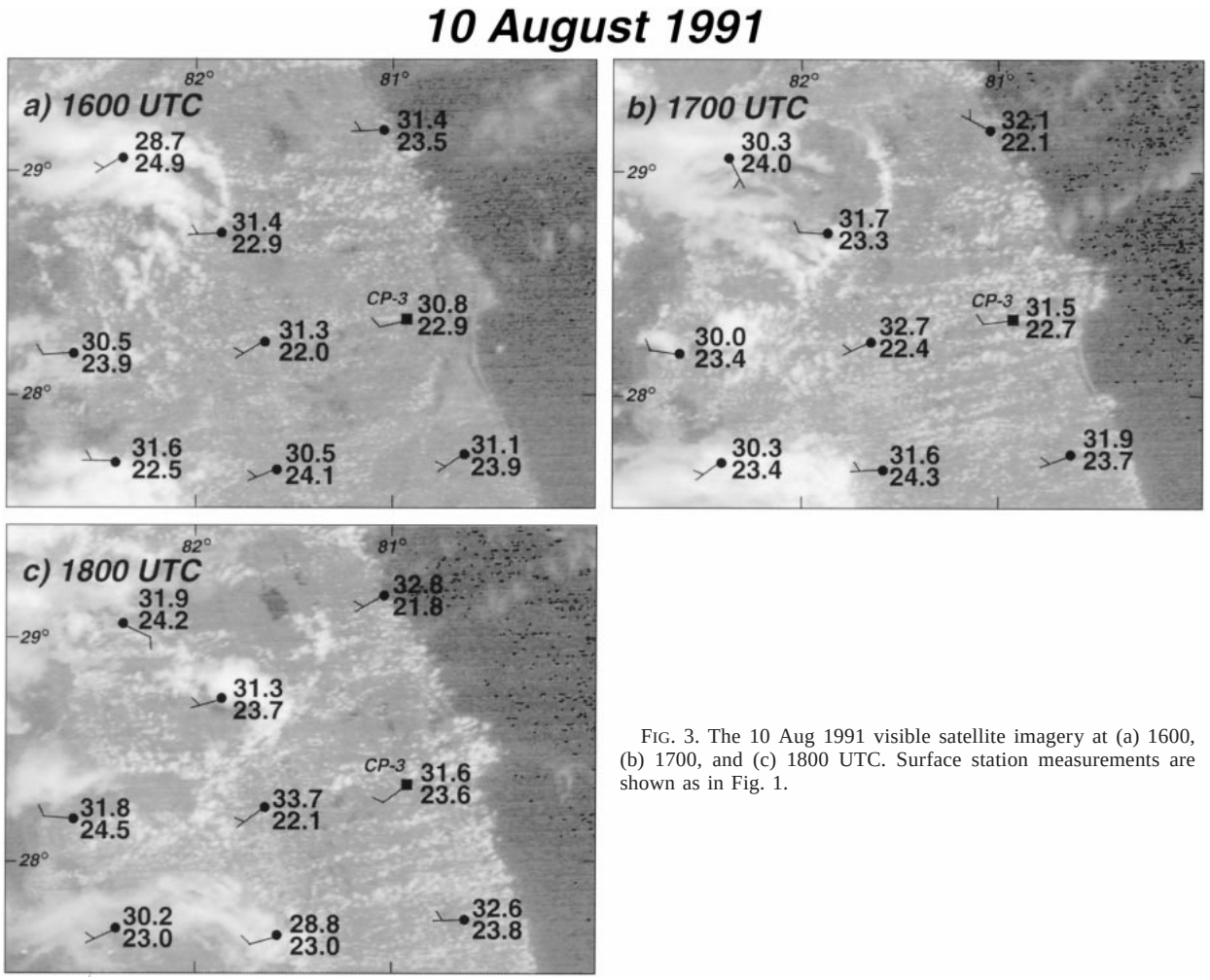

FIG. 3. The 10 Aug 1991 visible satellite imagery at (a) 1600, (b) 1700, and (c) 1800 UTC. Surface station measurements are shown as in Fig. 1.

the wind direction, are apparent north of CP-3 at 1600 (Fig. 3a). The low-level radar reflectivity field shows a suggestion of fine lines with an east–west orientation (Fig. 4a) and only a few clouds aloft (Fig. 4b). By 1700 the cloud streets cover more of the peninsula and a gust front propagates eastward across the state (Fig. 3b). Figure 4c shows that the reflectivity fine lines associated with the roll updraft branches are more pronounced and the roll spacing is wider than at 1600. The cloud streets atop the roll updraft branches with an east–west orientation are also more apparent (Fig. 4d).

At 1800 the cloud streets are still evident in the satellite imagery but no deep convection is forming near the CP-3 radar (Fig. 3c). Gust fronts continue to propagate eastward from convection generated in western Florida but there is no deep convection generated in advance of the outflow boundaries along the rolls alone. The radar reflectivity shows that the CBL convection is still predominately linear (Fig. 4e) and that the clouds are not deepening substantially (Fig. 4f). The maximum radar reflectivity of the echoes within the CaPE radar network does not exceed 20 dBZ_e throughout the day.

4. Influences on storm initiation

a. Thermodynamics

Numerous timely radiosondes were launched prior to and during thunderstorm formation. A sounding launched by mobile CLASS at 1657 on 29 July 1991 at the location of the balloon in Fig. 2c is shown in Fig. 5. Even though thunderstorms are forming less than 15 km away from the sounding site at this time, the sounding suggests that it is unlikely that thunderstorm formation will occur. First of all, the level of free convection (LFC) is at 2.3 km, well above the CBL depth of 0.8 km. The CBL depth was estimated from the height at which the moisture decreased in the sounding because this was generally more apparent than any other CBL measurement estimate. The virtual potential temperature profile is given on the right to show the ambiguity in measuring CBL depth. A conservative (i.e., low) estimate was used in these analyses. This estimate is consistent with the VAD reflectivity profiles (Weckwerth 1995). The roll circulations generally extend throughout the depth of the CBL (e.g., Faller and Kaylor 1966;

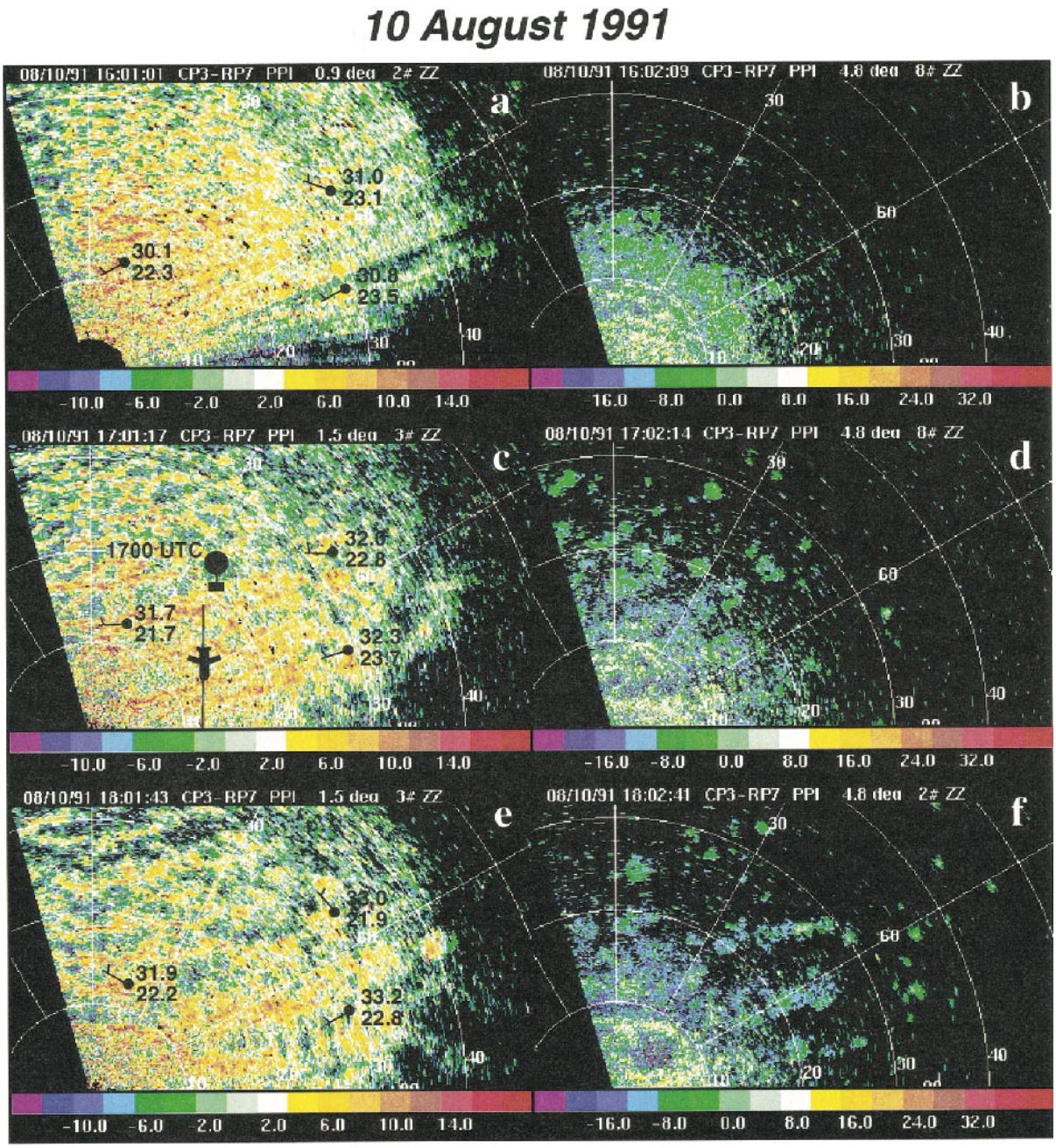

FIG. 4. Same as Fig. 2 except for 10 Aug 1991 showing no thunderstorm initiation by rolls. A Tico radiosonde was launched at 1700 UTC from the location of the balloon in (c). Sounding data will be shown in Fig. 6, along with aircraft data from the cross-roll direction between 1701 and 1724 UTC along the track shown in (c).

Doviak and Berger 1980; Rabin et al. 1982). The circulations may have some overshooting updrafts but it is unlikely that they could provide sufficient forcing to lift parcels up to 2.3 km. Furthermore, lifting a parcel with the mean moisture (14.6 g kg^{-1}) and potential temperature (302.6 K) of the lowest 50 mb produces a CAPE of only 644 J kg^{-1} with -30 J kg^{-1} of CIN to overcome.

Weckwerth et al. (1996) showed that when rolls are present, soundings may not measure the actual potential for convective instability. This is due to the fact that clouds, and hence thunderstorms, form in the roll updraft branches. Therefore it is necessary to measure the environmental parameters within these updraft regions to estimate the true potential for deep moist convection. The CaPE soundings were therefore modified using the UW and NCAR King Air aircraft data as they were flying in the cross-roll direction within the CBL on nu-

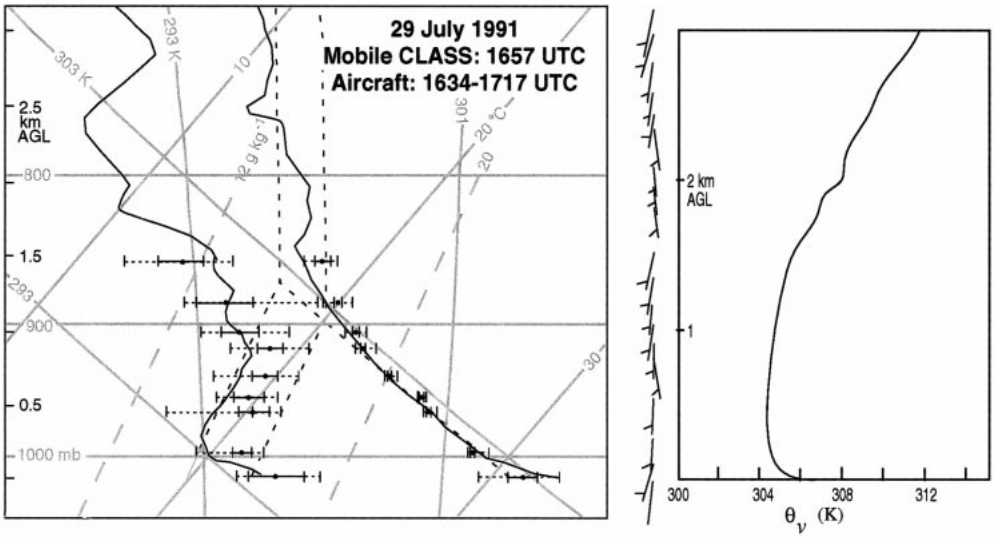

FIG. 5. The 29 Jul 1991 sounding from mobile CLASS at 1657 UTC from balloon location of Fig. 2c. The means and standard deviations of King Air–measured mixing ratios and potential temperatures are, respectively, shown by the dots and horizontal solid lines at numerous heights. The entire ranges of values observed are shown by the horizontal dashed lines. The lowest level depicts the mean, standard deviation, and maximum and minimum values obtained from a 30-min time series of PAM II data surrounding the launch and aircraft locations. The dotted gray lines indicate parcel ascents for sounding-measured air parcels and aircraft-measured roll updraft air parcels. Wind barbs are the same as in Fig. 1. The right panel illustrates the corresponding virtual potential temperature profile.

merous days. These data are overlaid in Fig. 5. The mean mixing ratios and potential temperatures observed at numerous heights are shown as dots on the sounding. The solid horizontal lines depict one standard deviation from the mean while the dashed extensions illustrate the entire range of values observed at the various levels. The surface levels show the comparable PAM II data for 30 min centered on the sounding launch time. Note that there is little variability in temperature throughout the CBL. The moisture values, however, show a significant amount of variability, consistent with the clear air roll results of Reinking et al. (1981) and Weckwerth et al. (1996).

The maximum moisture occurs within the roll updraft branches (Weckwerth et al. 1996). Clouds and perhaps thunderstorms occur atop these updraft branches. Thus if a parcel of air is lifted upward using the maximum CBL mixing ratio observed by the aircraft, then an accurate representation of convective potential is obtained. Using the 16.6 g kg^{-1} saturation mixing ratio line along with the 302.6-K dry adiabat for parcel ascent produces a new LFC of 1.2 km, virtually no negative area, and CAPE of 1665 J kg^{-1}. Given the estimate of CBL depth of 0.8 km, it is still not clear that rolls will lift parcels up to 1.2 km. Recall, however, that this is a conservative estimate of CBL depth and it is possibly higher when estimated from the virtual potential temperature profile. Furthermore, the lack of CIN makes it more likely that rolls can lift parcels to the LFC. Thus with this modification to the moisture profile, the sounding more likely supports convection initiation on 29 July (Fig. 5).

Figure 6 shows the comparable sounding on 10 August 1991, which was launched at 1700 from Tico Airport, as shown by the black balloon in Fig. 4c. This sounding examined on its own similarly, and accurately in this case, indicates that no thunderstorms are likely to form. The LFC is 2.3 km while the boundary layer depth is 0.85 km. Using the 15 g kg^{-1} saturation mixing ratio and 303.2 K dry adiabat, the CAPE is 966 J kg^{-1} with -44 J kg^{-1} of CIN to overcome before that convective potential may be achieved.

Modification of the 10 August 1700 sounding (Fig. 6) using the aircraft data warrants lifting parcels with mixing ratio values of 16.3 g kg^{-1} and the same potential temperature of 303.2 K. This produces a CIN of -18 J kg^{-1} and the CAPE is 1847 J kg^{-1}. This potential, however, cannot be achieved since the rolls, with an updraft depth of 0.85 km, cannot lift parcels to the LFC, which is 1.85 km. Thus even with the modification to the sounding, no thunderstorms would be expected on this day. These two examples on 29 July and 10 August suggest the insufficiency of utilizing single radiosondes alone to predict thunderstorm initiation due to rolls.

This favorable result of modifying the soundings using aircraft data is examined further using other CaPE cases. One of the comparisons is between CBL depth and the LFC (Fig. 7). It is suspected that environments with deeper CBLs, and therefore deeper roll updrafts, may more readily force air up to the LFC. If the rolls are deeper than the LFC on the storm days, then the majority of the closed circles should appear above and to the left of the one-to-one line of Fig. 7a. This does not occur. Although there is less difference between the

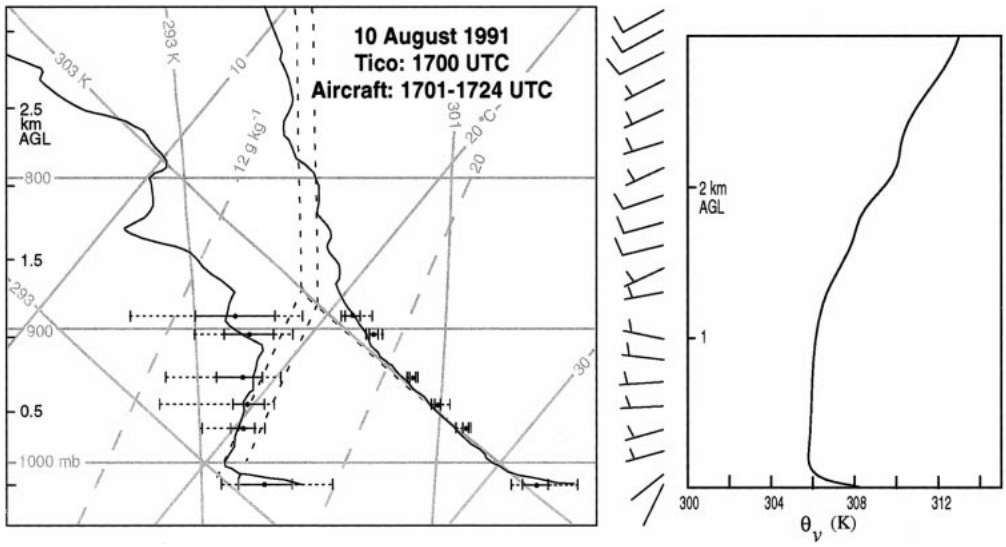

FIG. 6. Same as Fig. 5 except for 10 Aug 1991 sounding from Tico Airport from balloon location of Fig. 4c.

average CBL depth (z_i) and the average LFC on the storm (0.8-km difference) and no-storm days (1.3-km difference), it is not a robust predictor of whether or not storms will form.

Seven soundings were modified with CBL King Air measurements in a manner similar to that described with Figs. 5 and 6. This modified dataset is small due to the self-imposed requirement of having aircraft data within the same dual-Doppler lobe and within 30 min of the sounding launch time. Care was taken to ensure that the aircraft did not penetrate either the sea-breeze front or any developing cells. The labeled points in Fig. 7 represent those cases that met these requirements for modification; the dates and times for each label are provided in the figure caption. Figure 7b shows that the z_i − LFC difference between the storm (0.1-km difference) and no-storm days (1.2-km difference) is pronounced when the soundings are modified. Using the modified soundings, the storm cases are all near the one-to-one line on the scatterplot, as expected.

The stability of the soundings between the storm and no-storm days is also examined in terms of CAPE and

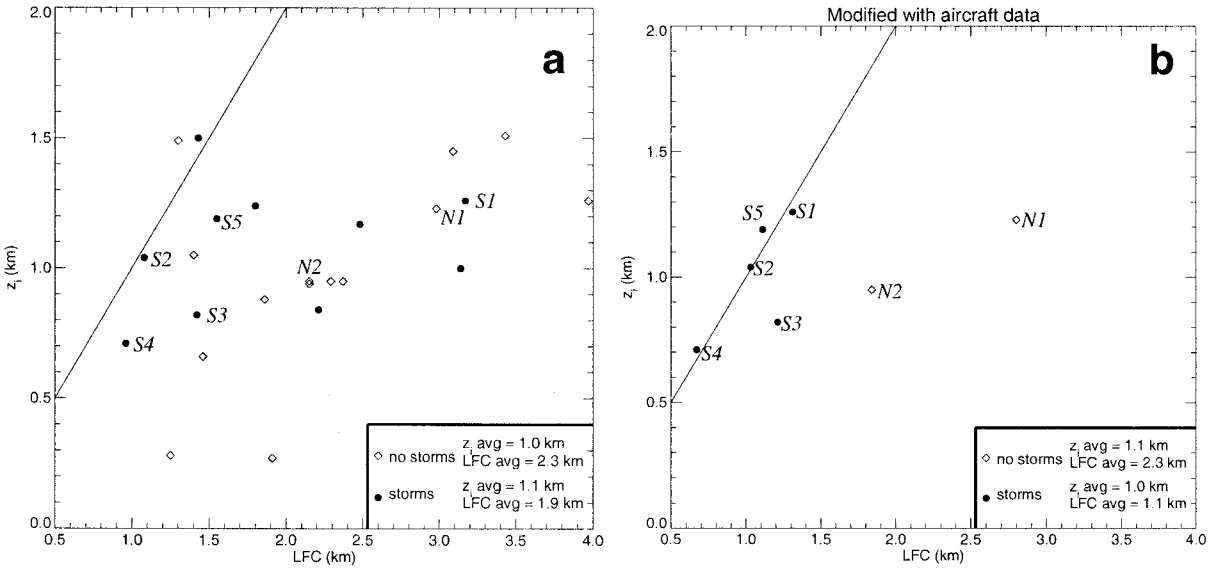

FIG. 7. Boundary layer depth (z_i; km) vs LFC (km) obtained from no-storm soundings (open diamonds) and storm soundings (filled circles). The one-to-one line is shown for reference. (b) A subset of that shown in (a) but modified to show the sounding stability parameters using the maximum mixing ratio values obtained within the roll updraft branches as the aircraft were flying normal to the roll axes. Labels indicate the no-storm and storm data points that were modified with aircraft data: N1 is 6 Aug 1800 UTC, N2 is 10 Aug 1700 UTC, S1 is 23 Jul 1823 UTC, S2 is 27 Jul 1600 UTC, S3 is 29 Jul 1657 UTC, S4 is 30 Jul 1421 UTC, and S5 is 2 Aug 1650 UTC.

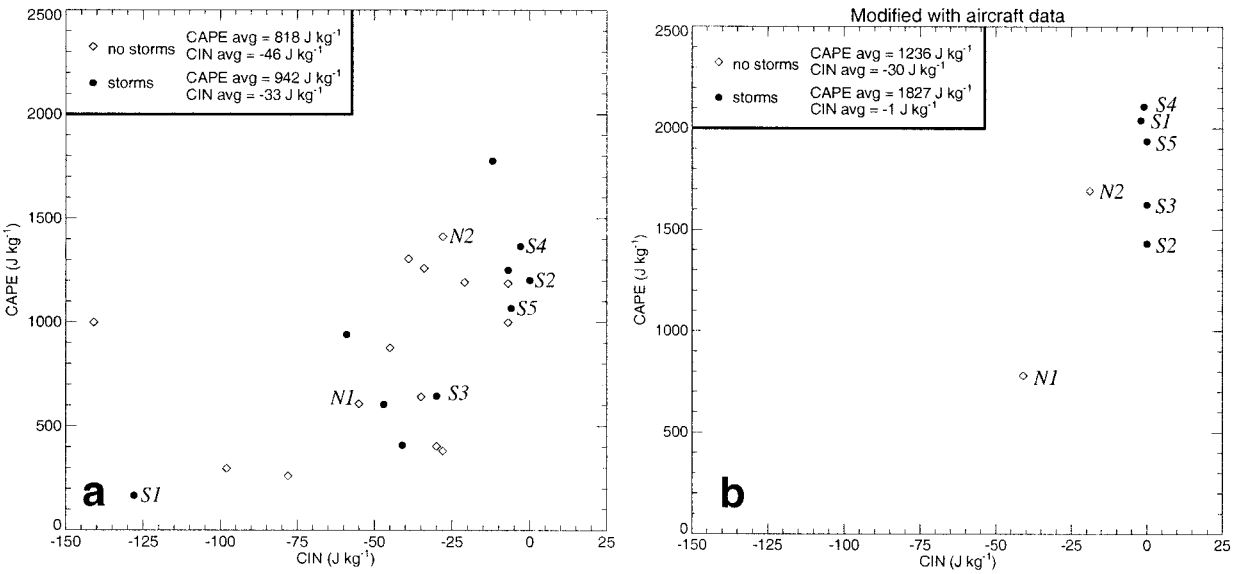

FIG. 8. CAPE (J kg^{-1}) vs negative area (CIN; J kg^{-1}) obtained from no-storm soundings (open diamonds) and storm soundings (filled circles). (b) A subset of that shown in (a) but modified to show the sounding stability parameters using the maximum mixing ratio values obtained within the roll updraft branches as the aircraft were flying normal to the roll axes. Labels are the same as in Fig. 7.

CIN. Colby (1984) showed that deep convection tends to occur where CIN is a minimum rather than where CAPE is a maximum. However, Fig. 8a shows that there is not a clustering of the original storm soundings occurring with low absolute values of CIN. Furthermore high CAPE values are not a robust indicator. It is true that the storm soundings have higher CAPEs and lower absolute values of CIN on the average; however, there is not an obvious difference between the two types of days for this to be used as a predictor of thunderstorm initiation. All of the modified storm cases, however, are clustered within the low CIN absolute value–high CAPE regime of Fig. 8b.

The midlevel moisture is also examined. The average relative humidity (RH) and mixing ratio in the layer between the lifting condensation level and 100 mb above it are calculated from the soundings. The results plotted in Fig. 9a show that the storm days do have slightly higher midlevel RH values; however, there are many no-storm days in the same region of high moisture

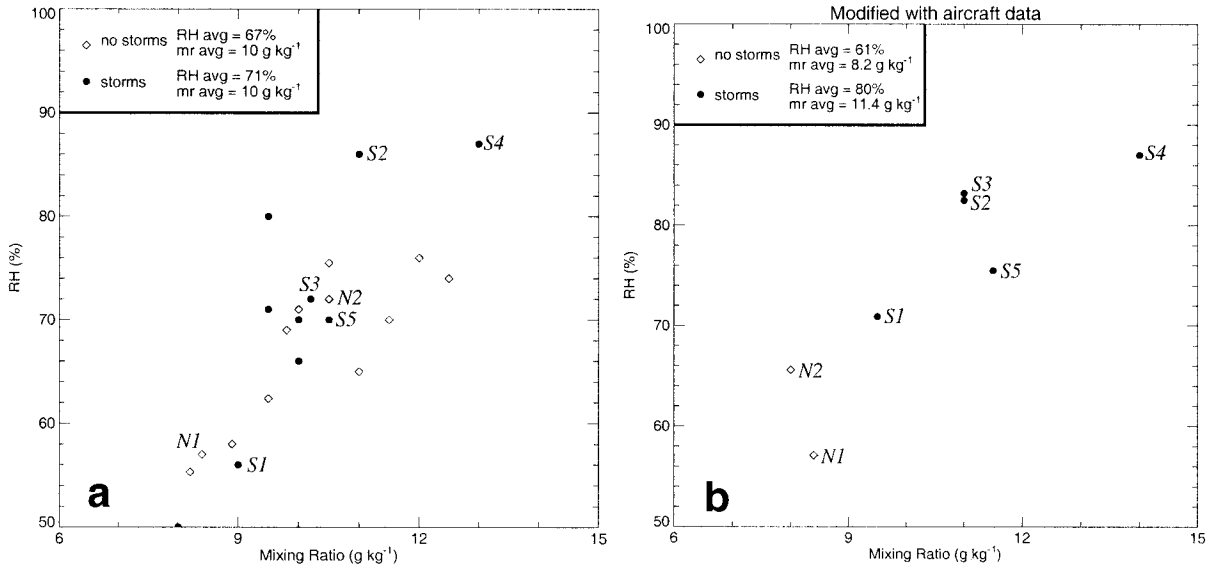

FIG. 9. Midlevel RH (%) vs midlevel mixing ratio (g kg^{-1}) obtained from no-storm soundings (open diamonds) and storm soundings (filled circles). (b) A subset of that shown in (a) but modified to show the sounding stability parameters using the maximum mixing ratio values obtained within the roll updraft branches as the aircraft were flying normal to the roll axes. Labels are the same as in Fig. 7.

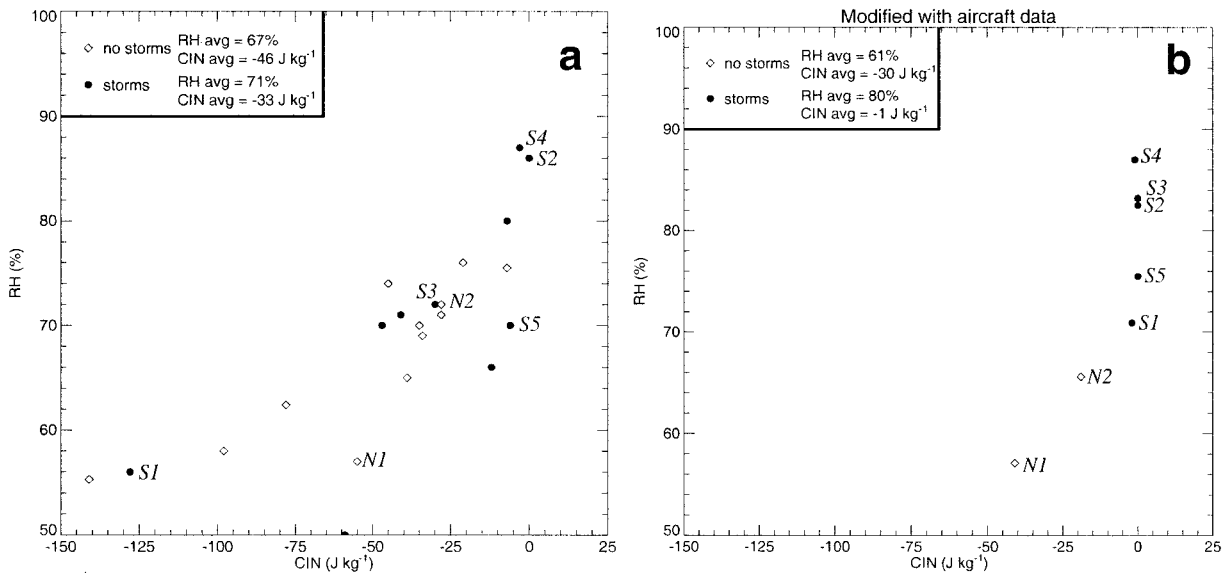

FIG. 10. Midlevel RH (%) vs negative area (CIN; J kg^{-1}) obtained from no-storm soundings (open diamonds) and storm soundings (filled circles). (b) A subset of that shown in (a) but modified to show the sounding stability parameters using the maximum mixing ratio values obtained within the roll updraft branches as the aircraft were flying normal to the roll axes. Labels are the same as in Fig. 7.

on the plot. Thus, once again, these original sounding measurements alone are not entirely effective in evaluating the likelihood of thunderstorm formation. When the soundings are modified with the aircraft measurements, however, all of the storm cases have higher midlevel moisture values than the no-storm cases (Fig. 9b).

Perhaps the most useful combination of original sounding parameters that suggests some utility in forecasting is the combination of midlevel RH and CIN (Fig. 10a). The majority of the storm days occur within the region of high moisture and low absolute values of CIN. There are, however, several no-storm examples in this same regime of high RH–low CIN absolute values, which implies that these sounding parameters alone are not sufficient to distinguish between storm and no-storm days. The modified soundings, once again, provide a clear distinction between the two types of days (Fig. 10b). On all seven days, an accurate indication of thunderstorm formation is obtained with the modified soundings.

b. PAM II data

The value of accurately measuring the moisture within the roll updraft branches above the surface layer is apparent when examining the PAM II variability. The 30-min means, standard deviations, and entire ranges of PAM station mixing ratios and potential temperatures are shown at the surface (i.e., lowest level) of each sounding (Figs. 5 and 6). Note that by modifying the sounding with as little as one standard deviation, as well as the maximum mixing ratios observed, thunderstorm initiation may be expected on both days. In fact, using the PAM II stations to modify the CaPE soundings incorrectly suggested that storms would form on all 13 days examined. During the CaPe project, the surface moisture content was generally very high but it was the moisture content of the updrafts within the CBL that, when combined with the temperature profile, was most useful for assessing the likelihood of thunderstorm formation.

In a further examination of the utility of PAM II data, 10-min temporal and three-station spatial averages were taken to obtain representative surface station measurements at times during which the rolls initiated deep convection and similar times on other days on which rolls developed but did not produce thunderstorms. Although not shown, neither surface mixing ratios, relative humidities, temperatures, potential temperatures, virtual potential temperatures, equivalent potential temperatures, wind speed, nor wind direction suggest any consistent difference between the storm and no-storm days.

c. Vertical wind shear

Although supercell thunderstorms require a great deal of shear (e.g., Browning 1964), airmass thunderstorms may readily exist within low-sheared environments (e.g., Byers and Braham 1949). These thunderstorms in the Florida summertime may be described as airmass thunderstorms; they are short lived and exist within low-shear environments. Although there is some horizontal variability, the thunderstorms are forming within one air mass. In fact, this may be one of the very few examples of true airmass thunderstorms since they do not form in association with typical boundaries separating air masses (e.g., gust fronts, sea-breeze fronts, cold fronts). Thus, not surprisingly, the shear did not have

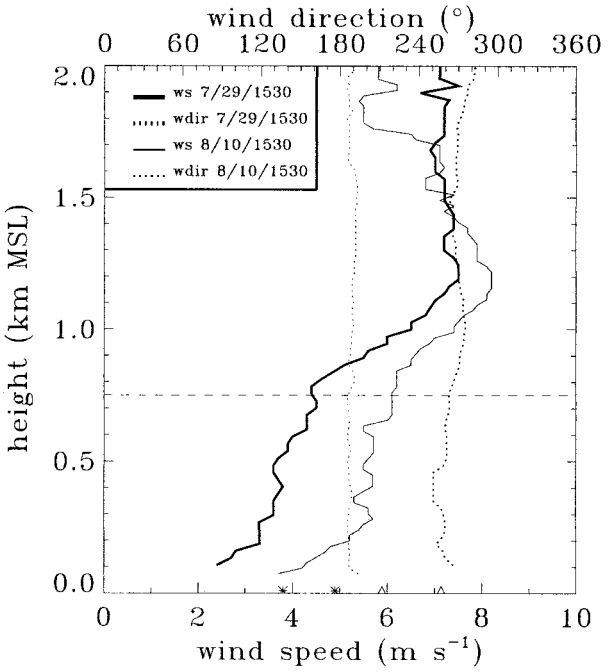

FIG. 11. VAD profiles of wind speed (m s^{-1}; solid lines) and direction (°; dashed lines) on 29 Jul at 1530 UTC (thick lines) just prior to thunderstorm initiation and on 10 Aug at 1530 UTC (thin lines), a day on which no deep convection was triggered by rolls. Stars and triangles at the surface indicate the 10-min average PAM II wind speed and direction, respectively, at CP-3.

any effect upon thunderstorms intensity (not shown). In addition, the balance between low-level environmental vorticity and the vorticity of a boundary shown to be important in creating an optimal state for convective development and sustenance was examined (Rotunno et al. 1988). This prediction from the theory of dry convection is irrelevant here since the shear is directed along the roll axes (i.e., along the boundaries).

The shear within and just atop the CBL was examined using the VAD technique since this technique produces more of a spatial average than the sounding winds (Browning and Wexler 1968). It seemed likely that the greater the shear directly atop the CBL, the less likelihood that the clouds could remain atop the roll updrafts. It was thought that if the small cells were influenced by the vertical wind shear and advected away from the roll updraft branches, they would lose their source of moisture and could not grow into thunderstorms. Examples of VAD profiles on the two days presented show virtually no difference in either the speed or direction profiles (Fig. 11). There is practically no shear whatsoever on any of the days examined. This was true for the entire CaPE project (Weckwerth et al. 1997), as well as the Small Cumulus Microphysical Study conducted in the same area during the summer of 1995 (Weckwerth et al. 1999a). Due to the virtual inexistence of shear, it is not surprising that an examination of the motion of cells atop the roll updraft branches showed that the cells always remained connected with the boundary layer roll updrafts, whether or not they eventually grew into thunderstorms. Thus the shear was not effective in predicting on which days rolls could initiate thunderstorms.

The formation of internal gravity waves within the inversion capping the CBL has been linked to the rolls acting as an obstacle to the flow in the presence of vertical wind shear. Clark et al. (1986) and Kuettner et al. (1987) showed that internal gravity waves may form atop the boundary layer when rolls impinge upon a sheared inversion layer. The lack of vertical wind shear within the CaPE dataset suggests that internal gravity waves were not likely to form atop the CBL. Thus the Balaji and Clark (1988) mechanism of internal gravity waves influencing convection initiation along rolls is not a likely factor in this dataset.

d. Surface topography

The locations of the first echoes were closely examined on all storm days to determine if surface features were influential in generating deep convection. These first echo positions appeared to be entirely random (not shown). The thunderstorms did not consistently form downwind of major water sources nor is there any significantly elevated terrain to provide additional forced vertical ascent. Thus, neither surface topography nor geography seemed to be a determinant in the initiation of deep convection by rolls.

As suggested in one-dimensional simulations of airmass thunderstorm initiation, soil moisture is a parameter that should be examined (Clark and Arritt 1995). Unfortunately the surface stations during CaPE did not have this capability. An evaluation of previous days' rainfall, however, did not show a clear indicator. Some prior days had measurable rainfall and produced storms on the following day while other preceding days had measurable rainfall and did not produce storms on the following day. Alternatively, days without measurable rainfall occurred prior to both storm and no-storm days. There was nothing in this dataset that suggested that antecedent rainfall was a clear indicator of convection initiation but soil moisture variations would be a good topic to examine with a proper dataset.

e. Three-dimensional wind fields

The magnitude of the roll circulations, the magnitude of the updrafts, and the depth of the updrafts were examined on the two different types of days utilizing the dual-Doppler wind fields obtained from CP-3 and CP-4 radars. The storm days were examined 15–30 min prior to thunderstorm development. There was not a significant difference between any of the three-dimensional wind fields (Weckwerth 1995). On both types of days, the horizontal vorticity due to the rolls is consistently $\sim 7 \times 10^{-3}$ s^{-1}, the updraft strength is typically ~ 1 m

s^{-1}, and the updraft depth is consistent with the CBL depth.

Furthermore the strength of the updrafts was estimated with the VAD analyses (not shown). The VAD vertical velocities were estimated by vertically integrating the divergence field. Average vertical velocities over a 10-km radius centered on the radar were consistently a few centimeters per second. There was no obvious variation between storm and no-storm days. The National Centers for Environmental Prediction–NCAR reanalysis data showed much the same. The large-scale vertical motion varied between -0.9 and $+0.3$ cm s^{-1} but there was no relationship between these values and thunderstorm initiation (not shown).

5. Summary and conclusions

It has been shown that rolls alone are capable of initiating deep convection, at least in a moist region such as Florida. The objective of this study was to determine the environmental difference between the storm and no-storm days. It was shown that the soundings alone are not sufficient in ascertaining the difference between storm and no-storm days. This is due to the fact that the majority of the soundings are not sampling the air within roll updraft branches. This updraft air is the air that will be lifted to form clouds and eventual thunderstorms.

In order to obtain an accurate representation of the potential for deep moist convection, soundings were modified using the King Air measurements as the aircraft were flying across the roll axes within the CBL. By modifying the soundings using the maximum CBL moisture observed, the LFC, CIN, and CAPE were recalculated. This new set of stability parameters accurately indicated on which days thunderstorms would occur on all seven days examined.

Further parameters were examined and showed no utility in assessing the difference between storm and no-storm days. The surface station data provided no effective indicators. The sounding- and VAD-measured vertical wind shear profiles, as well as cell motions relative to the roll updraft branches, showed no difference between the two types of days. There was no relationship between thunderstorm initiation and surface topography or geography. Details of the roll circulations were calculated using dual-Doppler techniques, specifically roll updraft depth and strength, and were found not to vary between storm and no-storm days.

The applicability of these results to regions other than the hot, humid climate of the Florida summertime should be addressed. It is possible that rolls in a drier region or during cold air outbreaks will produce a greater horizontal variation in temperature than in moisture (e.g., Atlas et al. 1986). Crook (1996) noted that variations in CBL temperature on the order of 1 K are actually more effective in influencing convection initiation. Thus it is possible that some of the same results would be obtained through modification of the soundings with the temperature values measured within the roll updraft. It must be noted that it is not the moisture variations themselves that are essential in evaluating thunderstorm development potential but rather the static stability of the atmosphere measured within the roll updraft regions.

It is believed that continuous monitoring of the depth and location of warm, moist updrafts within the CBL would be invaluable in forecasting thunderstorm formation. For nonsynoptically forced environments, it appears that the CBL water vapor and its variability must be more accurately measured if stability parameters are to be useful in thunderstorm initiation forecasting. Since horizontal variations on scales of 500 m must be sampled, the current radiosonde monitoring is insufficient. The Global Positioning System technology (e.g., Ware et al. 1996) has some potential for this application if the vertical resolution can be improved enough to retrieve numerous points within the CBL. Plans are under way for the water vapor sensing system (WVSS) to equip U.S. commercial aircraft with a water vapor sensing probe (Fleming 1996). If numerous measurements can be obtained within the CBL during takeoff and landing, the WVSS may be suitable for this application of sounding modification for the forecasting of convection initiation. Developing technology using scanning water vapor differential absorption lidar to obtain a three-dimensional mapping of the water vapor field also shows a great deal of promise for research applications (e.g., Wulfmeyer and Bösenberg 1998).

Plans are under way to field the International H_2O Project (IHOP 2002), which is intending to congregate all existing water vapor measuring sensors in the Southern Great Plains Clouds and Radiation Testbed area of Oklahoma and Kansas. One of the goals is to obtain a better understanding of the spatial and temporal scales needed for water vapor measurements to improve thunderstorm forecasting.

Acknowledgments. Much of the preliminary work on this topic was done as part of a dissertation with Roger Wakimoto (UCLA). Wakimoto and Jim Wilson (NCAR) also provided stimulating discussions on this topic, as well as detailed reviews of an earlier version of this paper. Dave Parsons (NCAR), Cindy Mueller (NCAR), Rob Cifelli (CSU), and one anonymous reviewer provided reviews that led to significant improvements of this manuscript. All of the radar, sounding, surface station, and King Air data were obtained from NCAR/ATD. Steve Williams (UCAR) provided the satellite imagery. Many thanks are bestowed upon the NCAR/ATD and UW field support personnel who so expertly collected data during CaPE.

REFERENCES

Asai, T., 1970a: Stability of a plane parallel flow with variable vertical shear and unstable stratification. *J. Meteor. Soc. Japan,* **48,** 129–139.

——, 1970b: Three-dimensional features of thermal convection in a plane Couette flow. *J. Meteor. Soc. Japan,* **48,** 18–29.
——, 1972: Thermal instability of a shear flow turning the direction with height. *J. Meteor. Soc. Japan,* **50,** 525–532.
Atkins, N. T., R. M. Wakimoto, and T. M. Weckwerth, 1995: Observations of the sea-breeze front during CaPE. Part II: Dual-Doppler and aircraft analysis. *Mon. Wea. Rev.,* **123,** 944–969.
Atlas, D., B. Walter, S.-H. Chou, and P. J. Sheu, 1986: The structure of the unstable marine boundary layer viewed by lidar and aircraft observations. *J. Atmos. Sci.,* **43,** 1301–1318.
Balaji, V., and T. L. Clark, 1988: Scale selection in locally forced convective fields and the initiation of deep cumulus. *J. Atmos. Sci.,* **45,** 3188–3211.
Brock, F. V., G. H. Saum, and S. R. Semmer, 1986: Portable automated mesonet II. *J. Atmos. Oceanic Technol.,* **3,** 573–582.
Browning, K. A., 1964: Airflow and precipitation trajectories within severe local storms which travel to the right of the winds. *J. Atmos. Sci.,* **21,** 634–639.
——, and H. Wexler, 1968: A determination of kinematic properties of a wind field using Doppler radar. *J. Appl. Meteor.,* **7,** 105–113.
Brümmer, B., 1985: Structure, dynamics, and energetics of boundary layer rolls from KonTur aircraft observations. *Contrib. Atmos. Phys.,* **58,** 237–254.
Byers, H. R., and H. R. Rodebush, 1948: Causes of thunderstorms of the Florida peninsula. *J. Meteor.,* **5,** 275–280.
——, and R. R. Braham Jr., 1949: *The Thunderstorm.* U.S. Govt. Printing Office, 287 pp.
Chlond, A., 1992: Three-dimensional simulation of cloud street development during a cold air outbreak. *Bound.-Layer Meteor.,* **58,** 161–200.
Christian, T. W., and R. M. Wakimoto, 1989: The relationship between radar reflectivities and clouds associated with horizontal roll convection on 8 August 1982. *Mon. Wea. Rev.,* **117,** 1530–1544.
Clark, C. A., and R. W. Arritt, 1995: Numerical simulations of the effect of soil moisture and vegetation cover on the development of deep convection. *J. Appl. Meteor.,* **34,** 2029–2045.
Clark, T. L., T. Hauf, and J. P. Kuettner, 1986: Convectively forced internal gravity waves: Results from two-dimensional numerical experiments. *Quart. J. Roy. Meteor. Soc.,* **112,** 899–925.
Colby, F. P., Jr., 1984: Convective inhibition as a predictor of convection during AVE-SESAME II. *Mon. Wea. Rev.,* **112,** 2239–2252.
Cole, H., and E. Miller, 1995: A correction for low-level radiosonde temperature and relative humidity measurements. Preprints, *Ninth Symp. on Meteorological Observations and Instrumentation,* Charlotte, NC, Amer. Meteor. Soc., 32–36.
——, and ——, 1999: Correction and re-calculation of humidity data from TOGA COARE radiosondes and development of humidity correction algorithms for global radiosonde data. *Proc. WCRP COARE-98 Conf.,* Boulder, CO, WCRP 107, WMO/TD-940, 139–141.
Crook, N. A., 1996: Sensitivity of moist convection forced by boundary layer processes to low-level thermodynamic fields. *Mon. Wea. Rev.,* **124,** 1767–1785.
Doviak, R. J., and M. Berger, 1980: Turbulence and waves in the optically clear planetary boundary layer resolved by dual-Doppler radars. *Radio Sci.,* **15,** 297–317.
Faller, A. J., 1963: An experimental study of the instability of the laminar Ekman boundary layer. *J. Fluid Mech.,* **15,** 560–576.
——, and R. E. Kaylor, 1966: A numerical study of the instability of the laminar Ekman boundary layer. *J. Atmos. Sci.,* **23,** 466–480.
Fankhauser, J. C., C. J. Biter, C. G. Mohr, and R. L. Vaughan, 1985: Objective analysis of constant altitude aircraft measurements in thunderstorm inflow regions. *J. Atmos. Oceanic Technol.,* **2,** 157–170.
——, N. A. Crook, J. Tuttle, L. J. Miller, and C. G. Wade, 1995: Initiation of deep convection along boundary layer convergence lines in a semitropical environment. *Mon. Wea. Rev.,* **123,** 291–313.
Fleming, R. J., 1996: The use of commercial aircraft as platforms for environmental measurements. *Bull. Amer. Meteor. Soc.,* **77,** 2229–2242.
Grossman, R. L., 1982: An analysis of vertical velocity spectra obtained in the BOMEX fair-weather, trade-wind boundary layer. *Bound.-Layer Meteor.,* **23,** 323–357.
Guichard, F., D. Parsons, and E. Miller, 2000: Thermodynamic and radiative impact of the correction of sounding humidity bias in the Tropics. *J. Climate,* **13,** 3611–3624.
Hane, C. E., H. B. Bluestein, T. M. Crawford, M. E. Baldwin, and R. M. Rabin, 1997: Severe thunderstorm development in relation to along-dryline variability: A case study. *Mon. Wea. Rev.,* **125,** 231–251.
Keeler, R. J., B. W. Lewis, R. K. Bowie, and J. R. Vinson, 1991: NCAR's C-band Doppler radars. Preprints, *25th Conf. on Radar Meteorology,* Paris, France, Amer. Meteor. Soc., 859–862.
Kingsmill, D. E., 1995: Convection initiation associated with a sea-breeze front, a gust front, and their collision. *Mon. Wea. Rev.,* **123,** 2913–2933.
Kristovich, D. A. R., 1993: Mean circulations of boundary-layer rolls in lake-effect snow storms. *Bound.-Layer Meteor.,* **63,** 293–315.
Kuettner, J. P., 1959: The band structure of the atmosphere. *Tellus,* **2,** 267–294.
——, 1971: Cloud bands in the earth's atmosphere. *Tellus,* **23,** 404–425.
——, P. A. Hildebrand, and T. L. Clark, 1987: Convection waves: Observations of gravity wave systems over convectively active boundary layers. *Quart. J. Roy. Meteor. Soc.,* **113,** 445–467.
Kuo, H. L., 1963: Perturbations of plane Couette flow in stratified fluid and origin of cloud streets. *Phys. Fluids,* **6,** 195–211.
Laird, N. F., D. A. R. Kristovich, R. M. Rauber, H. T. Ochs III, and L. J. Miller, 1995: The Cape Canaveral sea and river breezes: Kinematic structure and convective initiation. *Mon. Wea. Rev.,* **123,** 2942–2956.
Lauritsen, D. K., Z. Malekmadani, C. Morel, and R. McBeth, 1987: The Cross-chain Loran Atmospheric Sounding System (CLASS). Preprints, *Sixth Symp. on Meteorological Observations and Instrumentation,* New Orleans, LA, Amer. Meteor. Soc., 265–269.
LeMone, M. A., 1973: The structure and dynamics of horizontal roll vortices in the planetary boundary layer. *J. Atmos. Sci.,* **30,** 1077–1091.
——, and W. T. Pennell, 1976: The relationship of trade wind cumulus distribution to subcloud layer fluxes and structure. *Mon. Wea. Rev.,* **104,** 524–539.
Lilly, D. K., 1966: On the instability of Ekman boundary flow. *J. Atmos. Sci.,* **23,** 481–494.
Malkus, J. S., and H. Riehl, 1964: Cloud structure and distributions over the tropical Pacific Ocean. *Tellus,* **16,** 275–287.
Miura, Y., 1986: Aspect ratios of longitudinal rolls and convection cells observed during cold air outbreaks. *J. Atmos. Sci.,* **43,** 29–39.
Pielke, R., 1974: A three-dimensional numerical model of the sea breezes over south Florida. *Mon. Wea. Rev.,* **102,** 115–139.
Purdom, J. F. W., 1982: Subjective interpretation of geostationary satellite data for nowcasting. *Nowcasting,* K. A. Browning, Ed., Academic Press, 149–166.
Rabin, R. M., R. J. Doviak, and A. Sundara-Rajan, 1982: Doppler radar observations of momentum flux in a cloudless convective layer with rolls. *J. Atmos. Sci.,* **39,** 851–863.
Rasmussen, E. N., S. Richardson, J. M. Straka, P. M. Markowski, and D. O. Blanchard, 2000: The association of significant tornadoes with a baroclinic boundary on 2 June 1995. *Mon. Wea. Rev.,* **128,** 174–191.
Reinking, R. F., R. J. Doviak, and R. O. Gilmer, 1981: Clear-air roll vortices and turbulent motions as detected with an airborne gust probe and dual-Doppler radar. *J. Appl. Meteor.,* **20,** 678–685.
Rhea, J. O., 1966: A study of thunderstorm formation along dry lines. *J. Appl. Meteor.,* **5,** 58–63.

Rodi, A. R., J. C. Fankhauser, and R. L. Vaughan, 1991: Use of distance-measuring equipment (DME) for correcting biases in position, velocity and wind measurements from aircraft inertial navigation systems. *J. Atmos. Oceanic Technol.,* **8,** 827–834.

Rotunno, R., J. B. Klemp, and M. L. Weisman, 1988: A theory for strong, long-lived squall lines. *J. Atmos. Sci.,* **45,** 463–485.

Shapiro, M. A., T. Hampel, D. Rotzoll, and F. Mosher, 1985: Frontal hydraulic head: A microscale-α scale ($\sim$1 km) triggering mechanism for mesoconvective weather systems. *Mon. Wea. Rev.,* **113,** 1166–1183.

Stensrud, D. J., and H. N. Shirer, 1988: Development of boundary layer rolls from dynamic instabilities. *J. Atmos. Sci.,* **45,** 1007–1019.

Trier, S. B., D. B. Parsons, and J. H. E. Clark, 1991: Environment and evolution of a cold-frontal mesoscale convective system. *Mon. Wea. Rev.,* **119,** 2429–2455.

Wakimoto, R. M., and N. A. Atkins, 1994: Observations of the seabreeze front during CAPE. Part I: Single-Doppler, satellite, and cloud photogrammetry analysis. *Mon. Wea. Rev.,* **122,** 1092–1114.

Ware, R., and Coauthors, 1996: GPS sounding of the atmosphere: Preliminary results. *Bull. Amer. Meteor. Soc.,* **77,** 19–40.

Weckwerth, T. M., 1995: A study of horizontal convective rolls occurring within clear-air convective boundary layers. Cooperative Ph. D. Thesis 160, Dept. of Atmospheric Sciences, University of California, Los Angeles, and National Center for Atmospheric Research, 179 pp. [Available from UCLA, 405 Hilgard Ave., Los Angeles, CA 90095-1565.]

——, and R. M. Wakimoto, 1992: The initiation and organization of convective cells atop a cold-air outflow boundary. *Mon. Wea. Rev.,* **120,** 2169–2187.

——, J. W. Wilson, and R. M. Wakimoto, 1996: Thermodynamic variability within the convective boundary layer due to horizontal convective rolls. *Mon. Wea. Rev.,* **124,** 769–784.

——, ——, ——, and N. A. Crook, 1997: Horizontal convective rolls: Determining the environmental conditions supporting their existence and characteristics. *Mon. Wea. Rev.,* **125,** 505–526.

——, T. W. Horst, and J. W. Wilson, 1999a: An observational study of the evolution of horizontal convective rolls. *Mon. Wea. Rev.,* **127,** 2160–2179.

——, V. Wulfmeyer, R. M. Wakimoto, R. M. Hardesty, J. W. Wilson, and R. M. Banta, 1999b: NCAR–NOAA lower-tropospheric water vapor workshop. *Bull. Amer. Meteor. Soc.,* **80,** 2339–2357.

Wilson, J. W., and W. E. Schreiber, 1986: Initiation of convective storms by radar-observed boundary layer convergent lines. *Mon. Wea. Rev.,* **114,** 2516–2536.

——, and C. K. Mueller, 1993: Nowcasts of thunderstorm initiation and evolution. *Wea. Forecasting,* **8,** 113–131.

——, G. B. Foote, N. A. Crook, J. C. Fankhauser, C. G. Wade, J. D. Tuttle, C. K. Mueller, and S. K. Krueger, 1992: The role of boundary-layer convergence zones and horizontal rolls in the initiation of thunderstorms: A case study. *Mon. Wea. Rev.,* **120,** 1785–1815.

——, T. M. Weckwerth, J. Vivekanandan, R. M. Wakimoto, and R. W. Russell, 1994: Boundary layer clear-air radar echoes: Origin of echoes and accuracy of derived winds. *J. Atmos. Oceanic Technol.,* **11,** 1184–1206.

Woodcock, A. H., 1942: Soaring over the open sea. *Sci. Mon.,* **55,** 226–232.

Wulfmeyer, V., and J. Bösenberg, 1998: Ground-based differential absorption lidar for water-vapor profiling: Assessment of accuracy, resolution and meteorological applications. *Appl. Opt.,* **37,** 3825–3844.

Ziegler, C. L., and E. N. Rasmussen, 1998: The initiation of moist convection at the dryline: Forecasting issues from a case study perspective. *Wea. Forecasting,* **13,** 1106–1131.